iScience

CellPress
OPEN ACCESS

Article

Lack of thyroid hormone receptor beta is not detrimental for non-alcoholic steatohepatitis progression

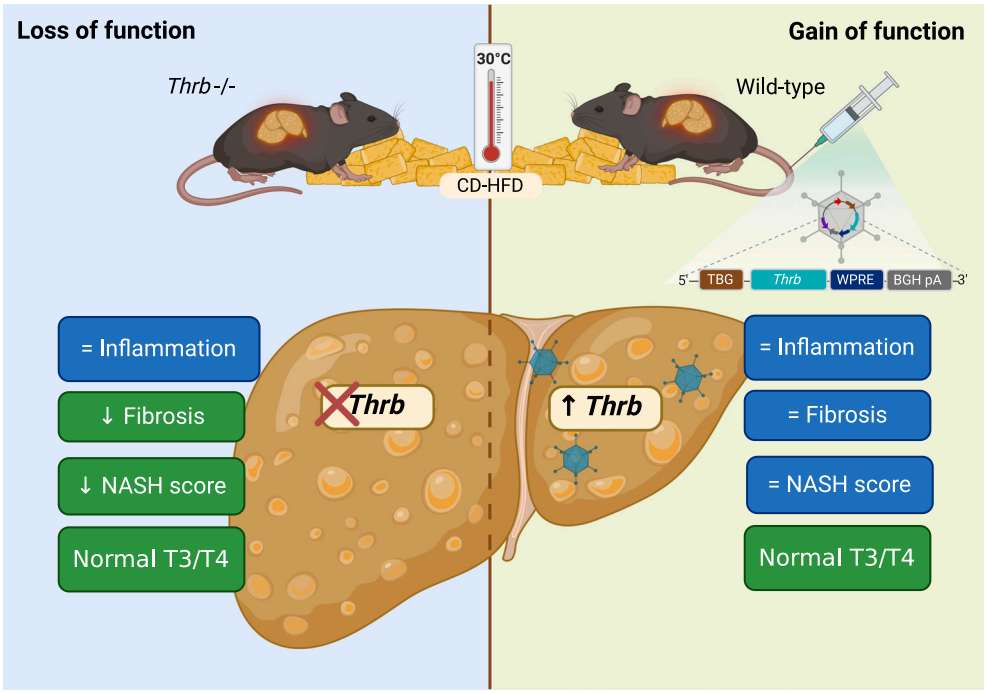

Nuria Lopez-Alcantara, Rebecca Oelkrug, Sarah Christine Sentis, Henriette Kirchner, Jens Mittag

Jens.Mittag@uni-luebeck.de

Highlights

Thermoneutral choline-deficient high-fat diet rapidly induces NASH without weight loss

Mice lacking TRβ do not develop NASH faster

Increasing hepatic TRβ expression by tail-vein AAV does not slow NASH progression

Lopez-Alcantara et al., iScience 26, 108064
October 20, 2023
https://doi.org/10.1016/j.isci.2023.108064

iScience

CellPress
OPEN ACCESS

Article

Lack of thyroid hormone receptor beta is not detrimental for non-alcoholic steatohepatitis progression

Nuria Lopez-Alcantara,[1] Rebecca Oelkrug,[1] Sarah Christine Sentis,[1] Henriette Kirchner,[2] and Jens Mittag[1,3,*]

SUMMARY

Agonists for thyroid hormone receptor β (TRβ) show promise in preclinical studies and clinical trials to improve non-alcoholic fatty liver disease. A recent study on human livers, however, revealed reduced TRβ expression in non-alcoholic steatohepatitis (NASH), indicating a developing thyroid hormone resistance, which could constitute a major obstacle for those agonists.

Using a rapid NASH paradigm combining choline-deficient high-fat diet and thermoneutrality, we confirm that TRβ declines during disease progression in mice similar to humans. Contrary to expectations, mice lacking TRβ showed less liver fibrosis, and NASH marker genes were not elevated. Conversely, increasing TRβ expression in wild-type NASH mice using liver-targeted gene therapy did not improve histology, gene expression, or metabolic parameters, indicating that TRβ receptor levels are of minor relevance for NASH development and progression in our model, and suggest that liver—rather than isoform—specificity might be more relevant for NASH treatment with thyroid hormone receptor agonists.

INTRODUCTION

Non-alcoholic fatty liver disease (NAFLD) is the most prevalent liver disease in Western countries, affecting around 30% of all adults.[1] NAFLD encompasses a wide spectrum of different stages, ranging from steatosis with normal hepatic function to non-alcoholic steatohepatitis (NASH) and further to cirrhosis and hepatocellular carcinoma.[2] Several external factors such as dietary choices are known to facilitate NAFLD development, but also endocrine alterations contribute to the development and progression of the disease.[3] Among those, thyroid hormones (THs) are most prominent, showing a strong correlation between lower circulating THs and NAFLD in humans.[4–6] Given the well-established beneficial effects of THs on cholesterol metabolism and hepatic lipid content,[7] activating hepatic TH signaling to improve liver health has been a holy grail in the field.[8] However, while a therapy with thyroxine (T4) does in fact reduce hepatic lipid content,[9] it carries the risk of undesired side effects including cardiovascular complications.[10] Therefore, strategies have been developed to specifically aim at targeting hepatic TH receptor β (TRβ), which delivered promising metabolic results,[11–16] but were either discontinued or have not reached clinical practice yet (NCT03900429).[17,18]

Recently, studies have shown that the local hepatic TH action might indeed be of greater relevance for disease pathogenesis than the systemic TH levels: a previous study on a small cohort in patients with NAFLD has found increased expression of the TH-inactivating enzyme deiodinase type 3 in human liver biopsies,[19] while another large cross-sectional study identified reduced expression of TRβ in livers of individuals with NASH.[20] Both studies suggest that with disease progression, the human liver might have reduced intracellular thyroid hormone action. Especially, the role of TRβ in this process might be crucial, as this isoform is the major regulator of hepatic lipid metabolism,[7,21] and a decline in the expression of this isoform might constitute a major obstacle in the current therapeutic strategies.

To characterize the role of available TRβ for NASH development, we established a novel rapid NASH induction protocol in mice and monitored disease progression in controls and animals lacking TRβ as loss-of-function model.[22,23] Most importantly, we performed our studies at thermoneutrality, which eliminates the cold stress on mice and makes them metabolically more comparable to humans. In addition, the endogenous hyperthyroidism of these TRβ knockout mice is normalized at this temperature, thus removing the high circulating TH levels acting on the intact TRα as confounding factor. Finally, as gain-of-function experiment, we restored TRβ expression using an adeno-associated virus (AAV)-based gene therapy in wild-type mice with NASH to test for metabolic benefits.

[1]Institut für Endokrinologie und Diabetes, AG Molekulare Endokrinologie, Universität zu Lübeck / Universitätsklinikum Schleswig-Holstein, Center for Brain Behavior and Metabolism CBBM, Ratzeburger Allee 160, 23562 Lübeck, Germany
[2]Institut für Humangenetik, AG Epigenetik und Metabolismus, Universität zu Lübeck / Universitätsklinikum Schleswig-Holstein, Center for Brain Behavior and Metabolism CBBM, Ratzeburger Allee 160, 23562 Lübeck, Germany
[3]Lead contact
*Correspondence: Jens.Mittag@uni-luebeck.de
https://doi.org/10.1016/j.isci.2023.108064

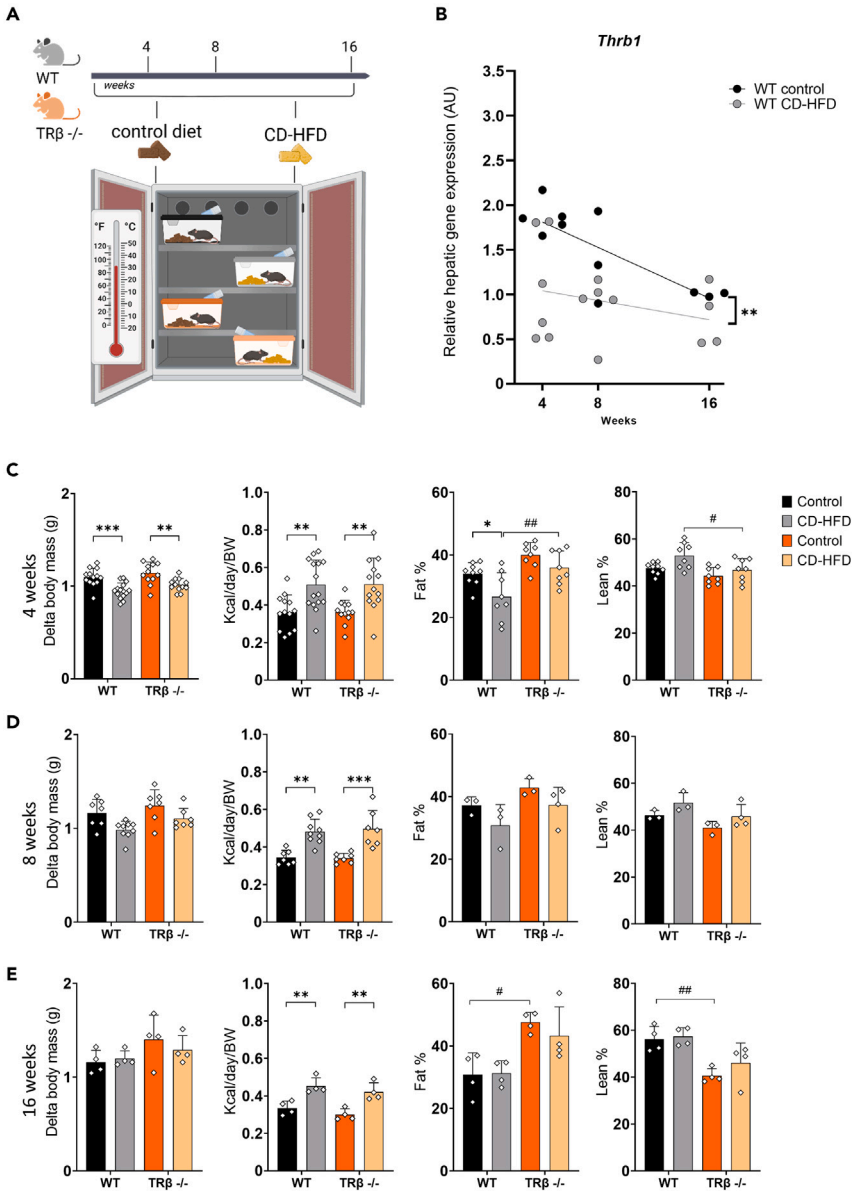

Figure 1. Effects of NASH diet on TRβ knockout mice

(A) Experimental overview.

(B) Effects of CD-HFD on *Thrb1* expression in wild-type mice.

(C–E) Body weight differences, food intake and body composition as assessed by NMR at 4, 8, and 16 weeks of age. Values are mean ± SD, *: $p < 0.05$; **: $p < 0.01$; ***: $p < 0.001$ for control vs. CD-HFD; #: $p < 0.05$; ##: $p < 0.01$ for wild-type vs. TRβ knockout (two-way ANOVA with Tukey's multiple comparison test, see Table S1).

RESULTS

To test whether impaired TRβ expression, as observed in human NASH liver,[20] would affect NASH development and progression, we put wild-type and TRβ knockout mice on a choline-deficient high-fat diet (CD-HFD). We chose to keep the animals at thermoneutrality for the duration of the experiment (Figure 1A), as this eliminates the elevated metabolism resulting from the permanent cold challenge at room temperature[24–26] and makes the animals more susceptible to metabolic challenges as demonstrated previously for NAFLD.[27] The animals were analyzed after 4, 8, and 16 weeks of diet. Similar to what observed in humans,[20] wild-type mice on CD-HFD showed lower *Thrb* expression than controls already at 4 weeks of diet, which became less pronounced at 8 and 16 weeks due to a general decline with increasing age (Figure 1B). Most remarkably, at thermoneutrality, the endogenously 2- to 3-fold elevated 3,3′,5-triiodothyronine (T3) and thyroxine (T4) levels of TRβ knockout mice[22,23] were almost normalized: Only a mild increase remained in total T4 at 8 weeks and 16 weeks (difference between

wild-type and TRβ knockout 26% at 8 weeks and 38% at 16 weeks, average of both diets), which however failed to reach significance in post hoc tests with the exception of the 16 weeks CD-HFD animals. T3 levels were not significantly different in any condition (difference between wild-type and TRβ knockout 40% at 4 weeks, 14% at 8 weeks, and 34% at 16 weeks, average of both diets). The diet itself had no significant effect on T3 or T4 serum levels (Figure S1A and Table S1). Similarly, there was little effect of the lack of TRβ on hepatic T3 or T4 levels, with the exception of a mild elevation in hepatic T4 at 4 weeks (difference between wild-type and TRβ knockout 47% at 4 weeks, 32% at 8 weeks, and 12% at 16 weeks, average of both diets). CD-HFD generally lowered hepatic T4 but not T3 levels (Figure S1B and Table S1). Nevertheless, the liver of TRβ knockout mice is still in a functionally hypothyroid state as evidenced by the lower deiodinase type I (*Dio1*) mRNA expression in these mice at 16 weeks, independent of the diet (Figure S1C).

After 4 weeks, a lower body weight gain was observed in CD-HFD animals as compared to control diet irrespective of the genotype, despite increased caloric intake. This difference was likely due to lower body fat mass as assessed by NMR (Figure 1C and Table S1), which however was still higher than the 17%–19% fat mass usually observed in wild-type males on chow diet at room temperature.[28] Over time, the initial differences in body weight and composition between the diets disappeared, while caloric intake remained higher (Figures 1D, 1E, and Table S1). After 16 weeks of diet, however, TRβ knockout mice exhibited higher fat and lower lean mass (Figure 1E, right panel), but normal C-peptide levels (Figure S1D).

When liver histology in those animals was studied using H&E staining, we observed moderate lipid deposition over the duration of the experiment in the control diet in both genotypes, while the animals on CD-HFD already had high lipid deposition at 4 weeks on the diet (Figure 2A). Overall, there was no obvious difference between the genotypes, which was additionally confirmed by oil red O quantification or direct measurement of hepatic lipid content (Figure S1E and S2A)—with the exception of more pronounced lipid deposition around the central vein in wild types at 4 weeks, which was not observed in TRβ knockout mice (Figure 2A). Serum levels of alanine transaminase and aspartate transaminase as indicators of hepatocyte damage were significantly elevated by the CD-HFD (Figure 2B), but again not different between the genotypes.

We then checked for signs of fibrosis using Sirius Red staining in these animals (Figure 3A). While mice on control diet show no obvious signs of fibrosis irrespective of the genotype, first signs of perisinusoidal collagen deposition were noticed at 8 weeks on CD-HFD in both genotypes. After 16 weeks of CD-HFD, there was marked pericellular and periportal fibrosis, indicative of full NASH; however, the fibrosis was less pronounced in TRβ knockout animals as compared to controls, which was confirmed by subsequent scoring (Figures 3B–3D first panel; Table S1). To further quantify NASH fibrosis and inflammation, we performed gene expression on *Col1a*, *Elf3*, and *Glis2* (Figures 3B–3D and Table S1) as well as *Tnfa*, *IL1β*, and *IL6* (Figure S2B) as established markers,[29] which revealed a significant induction of all genes except *IL1β* by the CD-HFD. While we did not find any effect of the genotype on *Glis2*, *Tnfa*, *IL6*, and *IL1β* mRNA expression, the lack of TRβ led to lower levels of *Col1a1* at 4 and 16 weeks as well as *Elf3* at 8 weeks (Figures 3B–3D and Table S1). Taken together, these data suggest that the lack of TRβ does not advance the progression of NASH in mice, and might even be protective against fibrosis development.

To test whether preventing the reduced *Thrb1* expression would elicit beneficial effects, we applied a gene therapy strategy in wild types on CD-HFD at thermoneutrality using tail-vein injection of an AAV8-expressing *Thrb1* or *mCherry* as control under the human TBG promoter to achieve liver specificity (Figure 4A). The AAV reached the liver as evidenced by the detection of the viral woodchuck hepatitis virus post-transcriptional regulatory element in genomic hepatic DNA (Figure S3A) and the prominent and widespread mCherry fluorescence in liver sections of the control animals (Figure S3B). The targeting approach successfully led to a 2-fold higher expression of *Thrb1* in the liver as compared to controls 4 weeks after AAV injection, while no increase was found in other organs such as the kidney (Figure 4B). When the animals with increased hepatic *Thrb1* expression were analyzed, we did not observe any change in T3/T4 ratio (Figure 4C), body weight, food intake or body composition (Figure 4D), or energy expenditure (Figure S3C). The liver histology revealed collagen deposition in the extracellular matrix indicative of NASH in both groups, which seemed more prominent in the *Thrb1* expression group, but did not reach significance (Figure 4E). Likewise, no significant changes were detected in gene expression of TH target genes or inflammation markers (Figures 4F and S3D) or hepatic T3 or T4 content (Figure S3E). The data therefore suggest that restoring *Thrb1* expression in NASH does not elicit beneficial effects for disease progression.

DISCUSSION

Our data show that the lack of TRβ does not facilitate NASH development and might even protect against fibrosis. Conversely, increasing *Thrb* expression in the livers of CD-HFD animals did not prevent disease progression. The data seem counterintuitive, given that TRβ agonists are clearly beneficial for hepatic parameters;[30] however, there are distinct molecular differences between altering ligand or receptor availability.

Benefits of thermoneutrality in our experimental paradigm

A decisive advantage of our NASH study is the use of thermoneutrality as experimental condition. It eliminates the constant cold challenge of small rodents at room temperature, which usually strongly induces metabolic rate,[24] and more closely mimics the human condition in several parameters including autonomic innervation.[24,26] Consequently, mice are more susceptible to metabolic challenges, which was shown previously for NAFLD development[27] and now demonstrated in our study for NASH. Given that some established NASH models can take up to a year of dietary intervention to develop fully at room temperature or are associated with weight loss as in methionine- and choline-deficient diets,[31,32] our novel experimental approach allows testing of therapeutical interventions in a reasonable time period. More importantly,

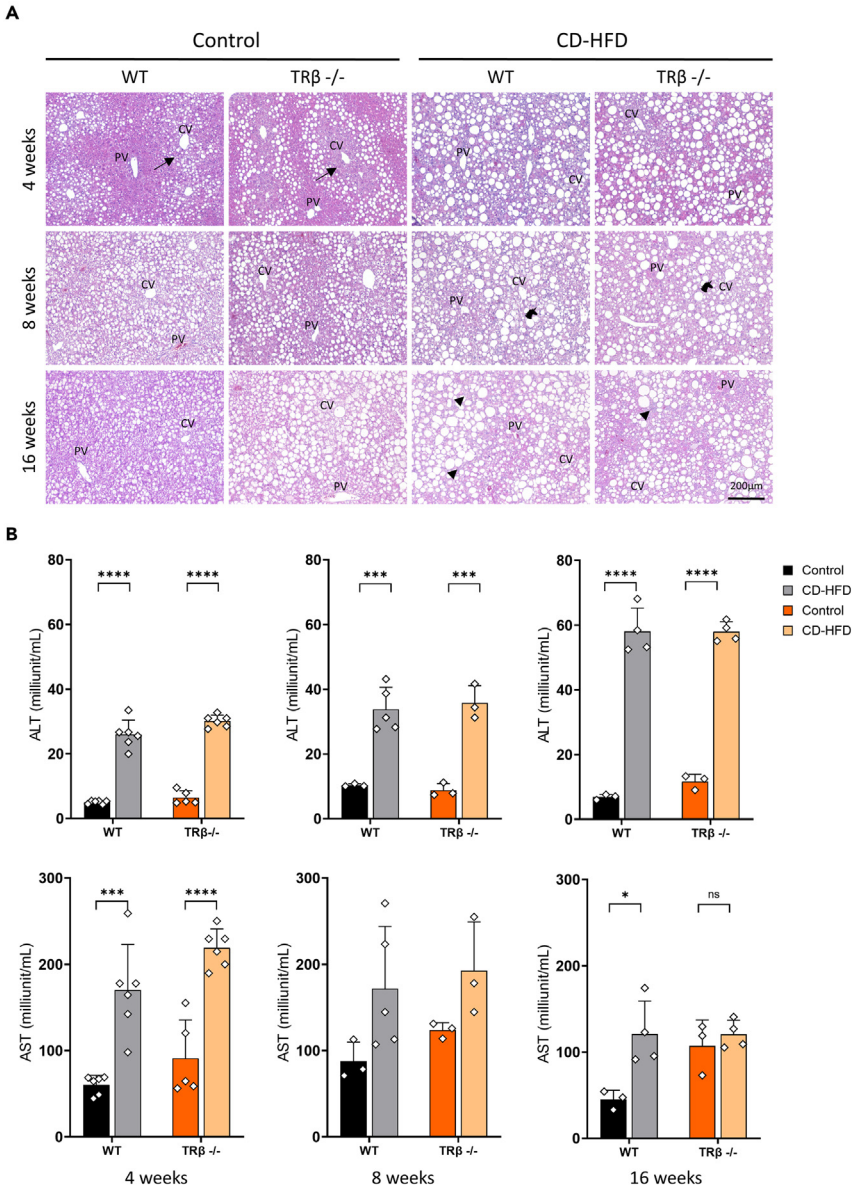

Figure 2. Histological effects of NASH diet on TRβ knockout mice

(A) Hepatic hematoxylin and eosin staining of wild types and TRβ knockout mice at 4, 8, and 16 weeks of CD-HFD or control diet. Central vein (CV); Portal vein (PV). Arrows indicate the difference in zonal lipid deposition between the genotypes. Arrowheads indicate invading immune cells. Unicorn heads indicate ballooning. Scale bar reflects 200 μm.

(B) Serum levels of alanine transaminase (ALT) and aspartate transaminase (AST) in these animals. Values are mean ± SD, *: $p < 0.05$; ***: $p < 0.001$; ****: $p < 0.0001$ for control vs. CD-HFD. (two-way ANOVA with Tukey's multiple comparison test, see Table S1).

thermoneutrality strongly alleviated the hyperthyroidism of TRβ knockout animals observed at room temperature,[22,23] which allowed studying the lack of TRβ without the confounding effects of a strong TRα1 activation in these animals. However, the lack of TRβ still confers a local hepatic hypothyroidism as can be seen from the repressed *Dio1* expression. Therefore, the experimental paradigm presented in this study provides interesting advantages for the fields of metabolic and thyroid research.

Differences between lower *Thrb* expression and thyroid hormone resistance in fatty liver disease

Most importantly, we were able to detect a reduced expression of *Thrb* in the livers of CD-HFD-treated wild-type mice, which progressed over time. This closely reflects the conditions found in human individuals with NASH in our previous study,[20] thus enabling us to use this model for molecular studies. Given the prominent effects of TRβ agonists for hepatic health,[30] our initial hypothesis was that reduced *Thrb* expression

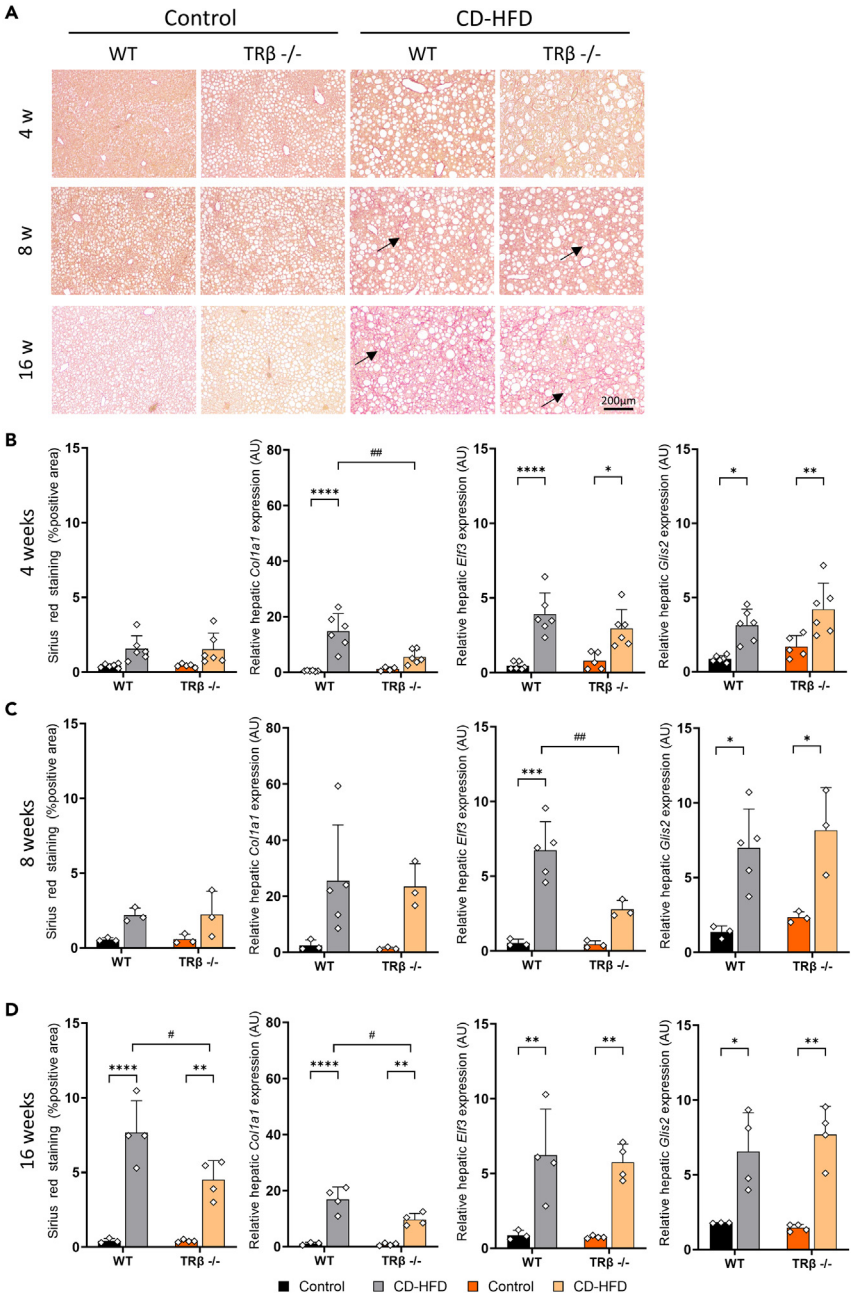

Figure 3. Signs of fibrosis and inflammation caused by NASH diet on TRβ knockout mice

(A) Hepatic Sirius red staining of wild types and TRβ knockout mice at 4, 8, and 16 weeks of CD-HFD or control diet. Scale bar reflects 200 µm.

(B–D) Quantification of Sirius red staining and hepatic gene expression of *Col1a1*, *Elf3*, and *Glis2* in these animals as assessed by qPCR. Values are mean ± SD, *: $p < 0.05$; **: $p < 0.01$; ***: $p < 0.001$; ****: $p < 0.0001$ for diet effect; #: $p < 0.05$; ##: $p < 0.01$ for genotype effect (two-way ANOVA with Tukey's multiple comparison test, see Table S1).

could cause hepatic thyroid hormone resistance, which would be detrimental for metabolic disorders. This is supported by findings in patients with resistance to thyroid hormone β (RTHβ) due to mutations in THRB, which present with increased hepatic lipid content[33], and animal models with a similar mutation that exhibit fatty liver due to elevated lipogenesis and reduced β-oxidation.[34] However, in these conditions, the TRβ is incapable of binding TH due to a mutation and remains in a permanently unliganded apo-receptor state, which can actively suppress gene expression and usually results in stronger phenotype than the lack of the receptor.[35,36] Moreover, it can be speculated that a mutant TRβ might interfere with the intact TRα1, e.g., by dimerization, while this would not occur in the absence or reduction of TRβ. Therefore, RTHβ due to THRB mutations cannot be directly compared to a condition of reduced TRβ as in NASH, as in the latter a compensation by

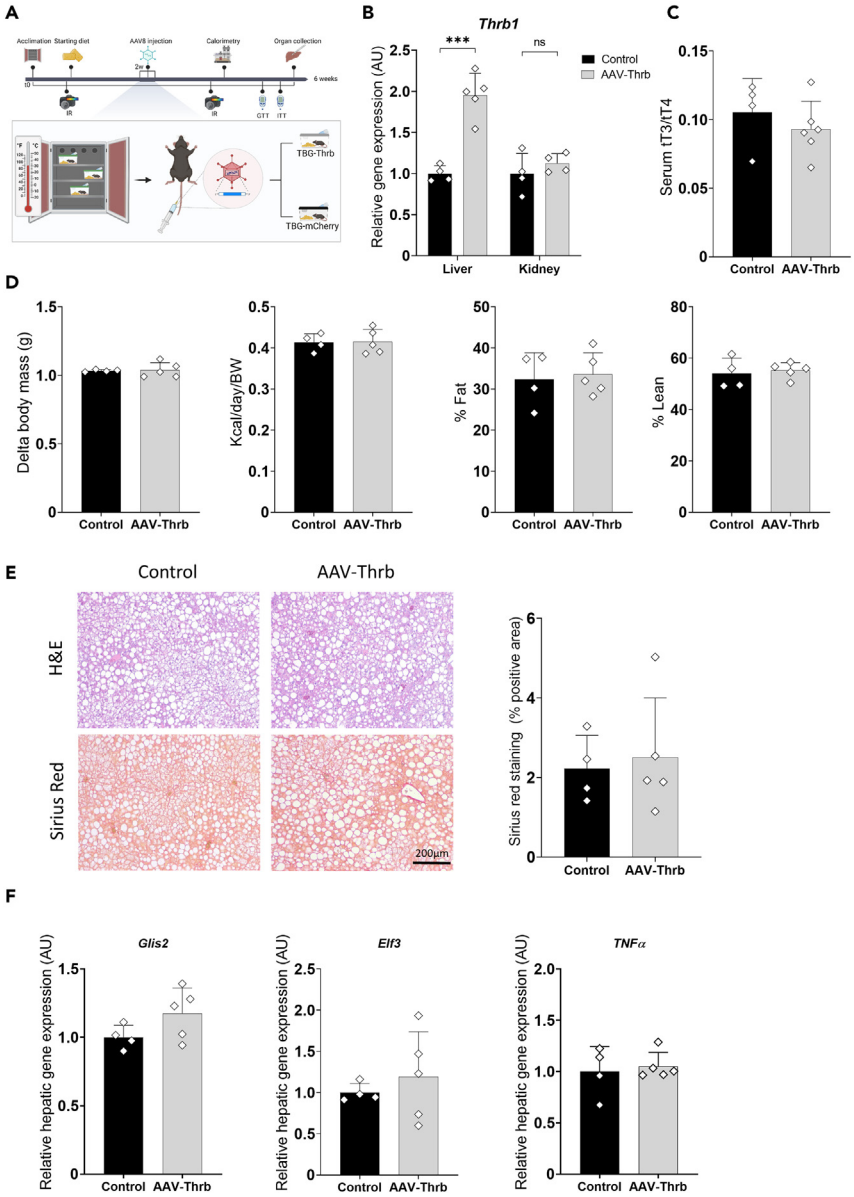

Figure 4. Reexpression of *Thrb1* in wild-type mice exposed to NASH diet

(A) Experimental paradigm depicting the time course of AAV8 tail-vein injection and analysis.

(B) Gene expression levels of *Thrb1* in liver and kidney of wild-type mice on CD-HFD injected with a control (black) or *Thrb1* expression construct (gray) under the TBG promoter.

(C) Serum total T3 to T4 ratio in these animals 6 weeks after starting the CD-HFD.

(D) Difference in body weight, food intake, or body composition in the animals.

(E) Hepatic hematoxylin and eosin as well as Sirius Red staining with quantification of fibrosis in these animals. Scale bar reflects 200 µm.

(F) Hepatic gene expression of *Glis2*, *Elf3*, and *TNFα* in the animals as assessed by qPCR. Values are mean ± SD, *: $p < 0.05$; **: $p < 0.01$; ***: $p < 0.001$ (unpaired Student's *t* test, see Table S1).

TRα1 is conceivable. Therefore, the use of a TRβ knockout instead of a model carrying a dominant-negative mutation to study NASH development is preferable, as it better reflects the conditions found in human NASH.[20]

Can TRα1 compensate TRβ in liver metabolism?

An absolute prerequisite for a compensation of TRβ by the other TR isoform TRα1 would be a co-expression of both receptors within the same cell. However, there is limited information available on the cellular distribution of TRs in the liver, given the problems of finding suitable

antibodies.[37] An initial study on protein level showed that both receptors are expressed in the liver, with higher levels around the central vein but a broader gradient for TRα.[38,39] A more recent study using single-cell RNA sequencing technology supported the presence of both TR isoforms in hepatocytes with only minor differences between perivenous and periportal areas and *Thrb* expression exceeding *Thra*.[40] A high-fat diet generally elevated the expression, but primarily increased the levels of *Thra* in immune cells.[40] This suggests that a reduction in *Thrb* expression could generally be compensated by the available TRα1 present in the same cell; however, given the perivenous-periportal expression gradient, this might not work equally well in all zones. In fact, when we investigated the liver histology in wild-type and TRβ knockout mice, we observed a striking difference in the zonation of lipid deposition in the early NAFLD, i.e., 4 weeks of control diet, which could result from altered β-oxidation, mitochondrial biogenesis, or autophagy—all established targets of hepatic TH action in mice.[41] This zonation effect, however, disappeared at later stages and under CD-HFD, suggesting that once the metabolic challenges build up, the liver is overwhelmed by lipids that are deposited without regard for localization. Given that the hepatic phenotype of TRβ knockout mice is not worse than in wild-type controls, this suggests that a compensation by TRα1 is generally possible in some aspects with minor region-specific differences in the early stages of NAFLD.

Conclusions

Given the plethora of results using TRβ-selective ligands,[18,30] it is undisputed that hepatic TH action is beneficial for liver metabolism. This is further supported by recent studies revealing that the initial increase in hepatic TH production through induction of *Dio1* inhibits NAFLD progression.[42] However, increasing hepatic TH action not only requires more ligand but also an available receptor. Our data now surprisingly demonstrate that the precise levels of *Thrb* are of minor importance: elevating *Thrb* expression is by itself not sufficient to provide metabolic benefits and vice versa a lack of TRβ in mouse NASH does not by itself promote disease progression, possibly by partial compensation through TRα1. Consequently, our findings suggest that it may be more relevant to focus on liver specificity for artificial TR ligands rather than TRβ selectivity—an aspect that is supported by recent studies highlighting the importance of TH transporters for directing these agonists to the liver.[43,44]

Limitations of the study

One of the limitations of our study is certainly the use of a global TRβ knockout, which allows the possibility that indirect consequences of TRβ deficiency in other organ systems, i.e., the autonomic nervous system or adipose tissue,[45–48] might affect the phenotype in our paradigm. Therefore, future studies could employ a hepatocyte-specific knockout or a liver targeting AAV-based approach, similar to what we used in the gain-of-function experiment. Here, it should be mentioned that, as we only provided qPCR data to show increased *Thrb* expression upon AAV transfection, we cannot quantify the resulting increase in protein, since we could not confirm the specificity of commercially available antibodies[49] using TRβ knockouts (see data availability for further information). Future studies should therefore include a tagged THRB to precisely quantify the levels of expression, identify the location of this receptor in the liver, and allow chromatin immunoprecipitation studies. Furthermore, given the zonation effects observed in the TRβ knockout animals, studies with greater cellular resolution by single-cell RNA sequencing will be required to pinpoint the precise contributions on the cellular level and to decipher the precise roles of the TR isoforms in NAFLD and NASH development and progression. Finally, while the NASH model developed in this study recapitulates histopathology and transcriptional characteristics of human NASH, it is not characterized by massive weight gain over the course of the diet and the choline deficiency of the diet could affect insulin sensitivity due to non-NASH-related effects.

STAR★METHODS

Detailed methods are provided in the online version of this paper and include the following:

- KEY RESOURCES TABLE
- RESOURCE AVAILABILITY
  - Lead contact
  - Materials availability
  - Data and code availability
- EXPERIMENTAL MODEL
  - Animals
  - AAV gene therapy
- METHOD DETAILS
  - Glucose and insulin tolerance test
  - Indirect calorimetry
  - qPCR
  - T3/T4 and C-peptide ELISA
  - Clinical chemistry parameters
  - Histology
- QUANTIFICATION AND STATISTICAL DETAILS

SUPPLEMENTAL INFORMATION

Supplemental information can be found online at https://doi.org/10.1016/j.isci.2023.108064.

ACKNOWLEDGMENTS

We thank the Gemeinsame Tierhaltung at the University of Lübeck for excellent animal caretaking. The technical support of Julia Resch from the University of Lübeck and An Ruiter and Marinne Frans from the Endocrine Laboratory Amsterdam UMC is greatly appreciated. We also appreciate the input of Timo Müller from the Helmholtz Munich for the development of the NASH model. The work was funded by the Deutsche Forschungsgemeinschaft (DFG) in the framework of the TRR296 "Local Control of Thyroid Hormone Action" to J.M. (Project-ID 424957847) and in an individual grant to R.O. (Project-ID 434396546). S.C.S. is a student of the DFG funded GRK1957 "Adipocyte-Brain-Crosstalk".

AUTHOR CONTRIBUTIONS

N.L.A., R.O., and S.C.S. conducted experiments; N.L.A., R.O., S.C.S., H.K., and J.M. analyzed the data; H.K. and J.M. supervised and designed the study; N.L.A. and J.M. drafted the manuscript. All authors discussed, corrected, and approved the manuscript.

DECLARATION OF INTERESTS

The authors declare no competing interests.

INCLUSION AND DIVERSITY

We support inclusive, diverse, and equitable conduct of research.

Received: April 10, 2023
Revised: September 14, 2023
Accepted: September 25, 2023
Published: September 28, 2023

REFERENCES

1. Younossi, Z.M., Golabi, P., Paik, J.M., Henry, A., Van Dongen, C., and Henry, L. (2023). The global epidemiology of nonalcoholic fatty liver disease (NAFLD) and nonalcoholic steatohepatitis (NASH): a systematic review. Hepatology *77*, 1335–1347. https://doi.org/10.1097/HEP.0000000000000004.
2. Michelotti, G.A., Machado, M.V., and Diehl, A.M. (2013). NAFLD, NASH and liver cancer. Nat. Rev. Gastroenterol. Hepatol. *10*, 656–665. https://doi.org/10.1038/nrgastro.2013.183.
3. Loria, P., Carulli, L., Bertolotti, M., and Lonardo, A. (2009). Endocrine and liver interaction: the role of endocrine pathways in NASH. Nat. Rev. Gastroenterol. Hepatol. *6*, 236–247. https://doi.org/10.1038/nrgastro.2009.33.
4. Ittermann, T., Haring, R., Wallaschofski, H., Baumeister, S.E., Nauck, M., Dörr, M., Lerch, M.M., Meyer zu Schwabedissen, H.E., Rosskopf, D., and Völzke, H. (2012). Inverse association between serum free thyroxine levels and hepatic steatosis: results from the Study of Health in Pomerania. Thyroid *22*, 568–574. https://doi.org/10.1089/thy.2011.0279.
5. Kim, D., Kim, W., Joo, S.K., Bae, J.M., Kim, J.H., and Ahmed, A. (2018). Subclinical Hypothyroidism and Low-Normal Thyroid Function Are Associated With Nonalcoholic Steatohepatitis and Fibrosis. Clin. Gastroenterol. Hepatol. *16*, 123–131.e1. https://doi.org/10.1016/j.cgh.2017.08.014.
6. Ludwig, U., Holzner, D., Denzer, C., Greinert, A., Haenle, M.M., Oeztuerk, S., Koenig, W., Boehm, B.O., Mason, R.A., Kratzer, W., et al. (2015). Subclinical and clinical hypothyroidism and non-alcoholic fatty liver disease: a cross-sectional study of a random population sample aged 18 to 65 years. BMC Endocr. Disord. *15*, 41. https://doi.org/10.1186/s12902-015-0030-5.
7. Sinha, R.A., Singh, B.K., and Yen, P.M. (2018). Direct effects of thyroid hormones on hepatic lipid metabolism. Nat. Rev. Endocrinol. *14*, 259–269. https://doi.org/10.1038/nrendo.2018.10.
8. Wirth, E.K., Puengel, T., Spranger, J., and Tacke, F. (2022). Thyroid hormones as a disease modifier and therapeutic target in nonalcoholic steatohepatitis. Expet Rev. Endocrinol. Metabol. *17*, 425–434. https://doi.org/10.1080/17446651.2022.2110864.
9. Bruinstroop, E., Dalan, R., Cao, Y., Bee, Y.M., Chandran, K., Cho, L.W., Soh, S.B., Teo, E.K., Toh, S.A., Leow, M.K.S., et al. (2018). Low-Dose Levothyroxine Reduces Intrahepatic Lipid Content in Patients With Type 2 Diabetes Mellitus and NAFLD. J. Clin. Endocrinol. Metab. *103*, 2698–2706. https://doi.org/10.1210/jc.2018-00475.
10. Dillmann, W. (2010). Cardiac hypertrophy and thyroid hormone signaling. Heart Fail. Rev. *15*, 125–132.
11. Berkenstam, A., Kristensen, J., Mellström, K., Carlsson, B., Malm, J., Rehnmark, S., Garg, N., Andersson, C.M., Rudling, M., Sjöberg, F., et al. (2008). The thyroid hormone mimetic compound KB2115 lowers plasma LDL cholesterol and stimulates bile acid synthesis without cardiac effects in humans. Proc. Natl. Acad. Sci. USA *105*, 663–667.
12. Cable, E.E., Finn, P.D., Stebbins, J.W., Hou, J., Ito, B.R., van Poelje, P.D., Linemeyer, D.L., and Erion, M.D. (2009). Reduction of hepatic steatosis in rats and mice after treatment with a liver-targeted thyroid hormone receptor agonist. Hepatology *49*, 407–417. https://doi.org/10.1002/hep.22572.
13. Caddeo, A., Kowalik, M.A., Serra, M., Runfola, M., Bacci, A., Rapposelli, S., Columbano, A., and Perra, A. (2021). TG68, a Novel Thyroid Hormone Receptor-beta Agonist for the Treatment of NAFLD. Int. J. Mol. Sci. *22*, 13105. https://doi.org/10.3390/ijms222313105.
14. Johansson, L., Rudling, M., Scanlan, T.S., Lundåsen, T., Webb, P., Baxter, J., Angelin, B., and Parini, P. (2005). Selective thyroid receptor modulation by GC-1 reduces serum lipids and stimulates steps of reverse cholesterol transport in euthyroid mice. Proc. Natl. Acad. Sci. USA *102*, 10297–10302.
15. Perra, A., Simbula, G., Simbula, M., Pibiri, M., Kowalik, M.A., Sulas, P., Cocco, M.T., Ledda-Columbano, G.M., and Columbano, A. (2008). Thyroid hormone (T3) and TRbeta agonist GC-1 inhibit/reverse nonalcoholic fatty liver in rats. Faseb. J. *22*, 2981–2989. https://doi.org/10.1096/fj.08-108464.
16. Vatner, D.F., Weismann, D., Beddow, S.A., Kumashiro, N., Erion, D.M., Liao, X.H., Grover, G.J., Webb, P., Phillips, K.J., Weiss, R.E., et al. (2013). Thyroid hormone receptor-beta agonists prevent hepatic steatosis in fat-fed rats but impair insulin sensitivity via discrete pathways. Am. J. Physiol. Endocrinol. Metab. *305*, E89–E100. https://doi.org/10.1152/ajpendo.00573.2012.
17. Harrison, S.A., Bashir, M., Moussa, S.E., McCarty, K., Pablo Frias, J., Taub, R., and Alkhouri, N. (2021). Effects of Resmetirom on Noninvasive Endpoints in a 36-Week Phase 2

Active Treatment Extension Study in Patients With NASH. Hepatol. Commun. *5*, 573–588. https://doi.org/10.1002/hep4.1657.

18. Harrison, S.A., Bashir, M.R., Guy, C.D., Zhou, R., Moylan, C.A., Frias, J.P., Alkhouri, N., Bansal, M.B., Baum, S., Neuschwander-Tetri, B.A., et al. (2019). Resmetirom (MGL-3196) for the treatment of non-alcoholic steatohepatitis: a multicentre, randomised, double-blind, placebo-controlled, phase 2 trial. Lancet *394*, 2012–2024. https://doi.org/10.1016/S0140-6736(19)32517-6.
19. Bohinc, B.N., Michelotti, G., Xie, G., Pang, H., Suzuki, A., Guy, C.D., Piercy, D., Kruger, L., Swiderska-Syn, M., Machado, M., et al. (2014). Repair-related activation of hedgehog signaling in stromal cells promotes intrahepatic hypothyroidism. Endocrinology *155*, 4591–4601. https://doi.org/10.1210/en.2014-1302.
20. Krause, C., Grohs, M., El Gammal, A.T., Wolter, S., Lehnert, H., Mann, O., Mittag, J., and Kirchner, H. (2018). Reduced expression of thyroid hormone receptor beta in human nonalcoholic steatohepatitis. Endocr. Connect. *7*, 1448–1456. https://doi.org/10.1530/EC-18-0499.
21. Gullberg, H., Rudling, M., Saltó, C., Forrest, D., Angelin, B., and Vennström, B. (2002). Requirement for thyroid hormone receptor beta in T3 regulation of cholesterol metabolism in mice. Mol. Endocrinol., Md *16*, 1767–1777.
22. Forrest, D., Erway, L.C., Ng, L., Altschuler, R., and Curran, T. (1996). Thyroid hormone receptor beta is essential for development of auditory function. Nat. Genet. *13*, 354–357.
23. Forrest, D., Hanebuth, E., Smeyne, R.J., Everds, N., Stewart, C.L., Wehner, J.M., and Curran, T. (1996). Recessive resistance to thyroid hormone in mice lacking thyroid hormone receptor beta: evidence for tissue-specific modulation of receptor function. EMBO J. *15*, 3006–3015.
24. Fischer, A.W., Cannon, B., and Nedergaard, J. (2018). Optimal housing temperatures for mice to mimic the thermal environment of humans: An experimental study. Mol. Metabol. *7*, 161–170. https://doi.org/10.1016/j.molmet.2017.10.009.
25. Fischer, A.W., Cannon, B., and Nedergaard, J. (2019). The answer to the question "What is the best housing temperature to translate mouse experiments to humans?" is: thermoneutrality. Mol. Metabol. *26*, 1–3. https://doi.org/10.1016/j.molmet.2019.05.006.
26. Swoap, S.J., Li, C., Wess, J., Parsons, A.D., Williams, T.D., and Overton, J.M. (2008). Vagal tone dominates autonomic control of mouse heart rate at thermoneutrality. Am. J. Physiol. Heart Circ. Physiol. *294*, H1581–H1588.
27. Giles, D.A., Moreno-Fernandez, M.E., Stankiewicz, T.E., Graspeuntner, S., Cappelletti, M., Wu, D., Mukherjee, R., Chan, C.C., Lawson, M.J., Klarquist, J., et al. (2017). Thermoneutral housing exacerbates nonalcoholic fatty liver disease in mice and allows for sex-independent disease modeling. Nat. Med. *23*, 829–838. https://doi.org/10.1038/nm.4346.
28. Oelkrug, R., Krause, C., Herrmann, B., Resch, J., Gachkar, S., El Gammal, A.T., Wolter, S., Mann, O., Oster, H., Kirchner, H., and Mittag, J. (2020). Maternal Brown Fat Thermogenesis Programs Glucose Tolerance in the Male Offspring. Cell Rep. *33*, 108351. https://doi.org/10.1016/j.celrep.2020.108351.
29. Loft, A., Alfaro, A.J., Schmidt, S.F., Pedersen, F.B., Terkelsen, M.K., Puglia, M., Chow, K.K., Feuchtinger, A., Troullinaki, M., Maida, A., et al. (2021). Liver-fibrosis-activated transcriptional networks govern hepatocyte reprogramming and intra-hepatic communication. Cell Metabol. *33*, 1685–1700.e9. https://doi.org/10.1016/j.cmet.2021.06.005.
30. Zucchi, R. (2020). Thyroid Hormone Analogues: An Update. Thyroid *30*, 1099–1105. https://doi.org/10.1089/thy.2020.0071.
31. Ipsen, D.H., Lykkesfeldt, J., and Tveden-Nyborg, P. (2020). Animal Models of Fibrosis in Nonalcoholic Steatohepatitis: Do They Reflect Human Disease? Adv. Nutr. *11*, 1696–1711. https://doi.org/10.1093/advances/nmaa081.
32. Porteiro, B., Fondevila, M.F., Buque, X., Gonzalez-Rellan, M.J., Fernandez, U., Mora, A., Beiroa, D., Senra, A., Gallego, R., Fernø, J., et al. (2018). Pharmacological stimulation of p53 with low-dose doxorubicin ameliorates diet-induced nonalcoholic steatosis and steatohepatitis. Mol. Metabol. *8*, 132–143. https://doi.org/10.1016/j.molmet.2017.12.005.
33. Moran, C., McEniery, C.M., Schoenmakers, N., Mitchell, C., Sleigh, A., Watson, L., Lyons, G., Burling, K., Barker, P., and Chatterjee, K. (2021). Dyslipidemia, Insulin Resistance, Ectopic Lipid Accumulation, and Vascular Function in Resistance to Thyroid Hormone beta. J. Clin. Endocrinol. Metab. *106*, e2005–e2014. https://doi.org/10.1210/clinem/dgab002.
34. Araki, O., Ying, H., Zhu, X.G., Willingham, M.C., and Cheng, S.Y. (2009). Distinct dysregulation of lipid metabolism by unliganded thyroid hormone receptor isoforms. Mol. Endocrinol. *23*, 308–315. https://doi.org/10.1210/me.2008-0311.
35. Ferrara, A.M., Onigata, K., Ercan, O., Woodhead, H., Weiss, R.E., and Refetoff, S. (2012). Homozygous thyroid hormone receptor beta-gene mutations in resistance to thyroid hormone: three new cases and review of the literature. J. Clin. Endocrinol. Metab. *97*, 1328–1336. https://doi.org/10.1210/jc.2011-2642.
36. Takeda, K., Sakurai, A., DeGroot, L.J., and Refetoff, S. (1992). Recessive inheritance of thyroid hormone resistance caused by complete deletion of the protein-coding region of the thyroid hormone receptor-beta gene. J. Clin. Endocrinol. Metab. *74*, 49–55. https://doi.org/10.1210/jcem.74.1.1727829.
37. Guan, W., Guyot, R., and Flamant, F. (2018). Two Protocols to Study the Interactions of Thyroid Hormone Receptors with Other Proteins and Chromatin. Methods Mol. Biol. *1801*, 9–16. https://doi.org/10.1007/978-1-4939-7902-8_2.
38. Zandieh Doulabi, B., Platvoet-ter Schiphorst, M., van Beeren, H.C., Labruyere, W.T., Lamers, W.H., Fliers, E., Bakker, O., and Wiersinga, W.M. (2002). TR(beta)1 protein is preferentially expressed in the pericentral zone of rat liver and exhibits marked diurnal variation. Endocrinology *143*, 979–984.
39. Zandieh-Doulabi, B., Dop, E., Schneiders, M., Schiphorst, M.P.T., Mansen, A., Vennström, B., Dijkstra, C.D., Bakker, O., and Wiersinga, W.M. (2003). Zonal expression of the thyroid hormone receptor alpha isoforms in rodent liver. J. Endocrinol. *179*, 379–385.
40. Park, S.R., Cho, C.S., Xi, J., Kang, H.M., and Lee, J.H. (2021). Holistic characterization of single-hepatocyte transcriptome responses to high-fat diet. Am. J. Physiol. Endocrinol. Metab. *320*, E244–E258. https://doi.org/10.1152/ajpendo.00391.2020.
41. Zhou, J., Tripathi, M., Ho, J.P., Widjaja, A.A., Shekeran, S.G., Camat, M.D., James, A., Wu, Y., Ching, J., Kovalik, J.P., et al. (2022). Thyroid Hormone Decreases Hepatic Steatosis, Inflammation, and Fibrosis in a Dietary Mouse Model of Nonalcoholic Steatohepatitis. Thyroid *32*, 725–738. https://doi.org/10.1089/thy.2021.0621.
42. Bruinstroop, E., Zhou, J., Tripathi, M., Yau, W.W., Boelen, A., Singh, B.K., and Yen, P.M. (2021). Early induction of hepatic deiodinase type 1 inhibits hepatosteatosis during NAFLD progression. Mol. Metabol. *53*, 101266. https://doi.org/10.1016/j.molmet.2021.101266.
43. Hönes, G.S., Sivakumar, R.G., Hoppe, C., König, J., Führer, D., and Moeller, L.C. (2022). Cell-Specific Transport and Thyroid Hormone Receptor Isoform Selectivity Account for Hepatocyte-Targeted Thyromimetic Action of MGL-3196. Int. J. Mol. Sci. *23*, 13714. https://doi.org/10.3390/ijms232213714.
44. Kersseboom, S., van Gucht, A.L.M., van Mullem, A., Brigante, G., Farina, S., Carlsson, B., Donkers, J.M., van de Graaf, S.F.J., Peeters, R.P., and Visser, T.J. (2017). Role of the Bile Acid Transporter SLC10A1 in Liver Targeting of the Lipid-Lowering Thyroid Hormone Analog Eprotirome. Endocrinology *158*, 3307–3318. https://doi.org/10.1210/en.2017-00433.
45. Hameed, S., Patterson, M., Dhillo, W.S., Rahman, S.A., Ma, Y., Holton, C., Gogakos, A., Yeo, G.S.H., Lam, B.Y.H., Polex-Wolf, J., et al. (2017). Thyroid Hormone Receptor Beta in the Ventromedial Hypothalamus Is Essential for the Physiological Regulation of Food Intake and Body Weight. Cell Rep. *19*, 2202–2209. https://doi.org/10.1016/j.celrep.2017.05.066.
46. Johann, K., Cremer, A.L., Fischer, A.W., Heine, M., Pensado, E.R., Resch, J., Nock, S., Virtue, S., Harder, L., Oelkrug, R., et al. (2019). Thyroid-Hormone-Induced Browning of White Adipose Tissue Does Not Contribute to Thermogenesis and Glucose Consumption. Cell Rep. *27*, 3385–3400.e3. https://doi.org/10.1016/j.celrep.2019.05.054.
47. Klieverik, L.P., Janssen, S.F., van Riel, A., Foppen, E., Bisschop, P.H., Serlie, M.J., Boelen, A., Ackermans, M.T., Sauerwein, H.P., Fliers, E., and Kalsbeek, A. (2009). Thyroid hormone modulates glucose production via a sympathetic pathway from the hypothalamic paraventricular nucleus to the liver. Proc. Natl. Acad. Sci. USA *106*, 5966–5971.
48. Obregon, M.J. (2014). Adipose tissues and thyroid hormones. Front. Physiol. *5*, 479. https://doi.org/10.3389/fphys.2014.00479.
49. Ohba, K., Sinha, R.A., Singh, B.K., Iannucci, L.F., Zhou, J., Kovalik, J.P., Liao, X.H., Refetoff, S., Sng, J.C.G., Leow, M.K.S., and Yen, P.M. (2017). Changes in Hepatic TRbeta Protein Expression, Lipogenic Gene Expression, and Long-Chain Acylcarnitine Levels During Chronic Hyperthyroidism and Triiodothyronine Withdrawal in a Mouse

Model. Thyroid *27*, 852–860. https://doi.org/10.1089/thy.2016.0456.

50. Heldmaier, G. (1975). The influence of the social thermoregulation on the cold-adaptive growth of BAT in hairless and furred mice. Pflügers Archiv *355*, 261–266. https://doi.org/10.1007/bf00583688.
51. Dore, R., Watson, L., Hollidge, S., Krause, C., Sentis, S.C., Oelkrug, R., Geißler, C., Johann, K., Pedaran, M., Lyons, G., et al. (2023). Resistance to thyroid hormone induced tachycardia in RTHalpha syndrome. Nat. Commun. *14*, 3312. https://doi.org/10.1038/s41467-023-38960-1.
52. Nicolaisen, T.S., Klein, A.B., Dmytriyeva, O., Lund, J., Ingerslev, L.R., Fritzen, A.M., Carl, C.S., Lundsgaard, A.M., Frost, M., Ma, T., et al. (2020). Thyroid hormone receptor alpha in skeletal muscle is essential for T3-mediated increase in energy expenditure. FASEB J. *34*, 15480–15491. https://doi.org/10.1096/fj.202001258RR.
53. Boelen, A., van der Spek, A.H., Bloise, F., de Vries, E.M., Surovtseva, O.V., van Beeren, M., Ackermans, M.T., Kwakkel, J., and Fliers, E. (2017). Tissue thyroid hormone metabolism is differentially regulated during illness in mice. J. Endocrinol. *233*, 25–36. https://doi.org/10.1530/JOE-16-0483.

STAR★METHODS

KEY RESOURCES TABLE

REAGENT or RESOURCE	SOURCE	IDENTIFIER
Antibodies		
Donkey anti-Goat antibody, Alexa Fluor™ 594	Invitrogen	Cat#A11058; RRID: AB_2534105
Goat polyclonal anti-mCherry antibody	OriGene Technologies GmbH	Cat#AB0040; RRID: AB_2333093
Bacterial and virus strains		
AAV8-TBG-mCherry	VectorBuilder GmbH	N/A
AAV8-TBG-mThrb1	VectorBuilder GmbH	N/A
Chemicals, peptides, and recombinant proteins		
2-propanol	Carl Roth GmbH&Co KG	Cat#CP41.3
Acetic acid	Carl Roth GmbH&Co KG	Cat#3738.4
cOmplete Protease Inhibitor Cocktail	Roche	Cat#5892970001
D-(+)-Glucose	Sigma-Aldrich	Cat#G7021
Direct Red 80	Sigma-Aldrich	Cat#365548
FastStart Universal SYBR Green Master Mix (+ROX)	Roche	Cat# 04913914001
Histoplast Paraffin Wax	Thermo Fisher Scientific (Thermo Scientific)	Cat#6774060
Insulin (NovoRapid Penfill 100E/ml)	Novo Nordisk	Cat#00558713
Mounting medium, Aqueous, BioAssay	USBiological	Cat#M4679-01
Oil Red O	Sigma-Aldrich	Cat#O0625
Paraformaldehyde 4%	Thermo Fisher Scientific (Thermo Scientific)	Cat#J19943-K2
Picric aqueous solution 1.2%	AppliChem GmbH	Cat#A2520
ProLong TM Diamond Antifade Mountant with DAPI	Invitrogen	Cat#P36971
Qiazol Lysis Reagent	QIAGEN	Cat#74704
Xylol	Carl Roth GmbH&Co KG	Cat#9713.3
Critical commercial assays		
Alanine Aminotransferase (ALT) Activity Assay	Sigma-Aldrich	Cat#MAK052
Aspartate Aminotransferase (AST) Activity Assay	Sigma-Aldrich	Cat#MAK055
Eosin Y solution 0.5% aqueous	Carl Roth GmbH&Co KG	Cat#X883.2
Mayer's hemalum solution	Sigma-Aldrich	Cat#1.09249
miRNeasy Mini Kit	QIAGEN	CAT#217084
Molecular Biology RevertAid Strand cDNA Kit	Thermo Fisher Scientific (Thermo Scientific)	Cat# K1622
Rat/Mouse C-Peptide 2 ELISA	Sigma-Aldrich	Cat#EZRMCP2-21K
Serum total T3	NovaTec Immundiagnostica GmbH	Cat#DNOV053
Serum total T4	DRG Diagnostics	Cat#EIA-1781
Triglyceride Quantification Kit	Sigma-Aldrich	Cat#MAK266
Experimental models: Organisms/strains		
C57BL/6NCrl mice	Charles River Laboratories (breeding colony in Germany)	RRID:MGI:2160593
Choline-deficient high fat diet (CD-HFD)	ssniff Spezialdiäten GmbH	Cat#S0585-E010
Control diet (CSAA)	ssniff Spezialdiäten GmbH	Cat#E15668-043
B6.129S1-Thrbtm1Df/J (TRβ ko)	Forrest et al., 1996	RRID:IMSR_JAX:003462

(*Continued on next page*)

Continued

REAGENT or RESOURCE	SOURCE	IDENTIFIER
Oligonucleotides		
Primer: Col1a1 Forward: GCTCCTCTTAGGGGCCACT Reverse: CCACGTCTCACCATTGGGG	Integrated DNA Technologies Germany GmbH	N/A
Primer: Dio1 Forward: GCTGAAGCGGCTTGTGATATT Reverse: GTTGTCAGGGGCGAATCGG	Integrated DNA Technologies Germany GmbH	N/A
Primer: Elf3 Forward: GCTGCCACCTGTGAGATCAG Reverse: GTGCCAAAGGTAGTCGGAGG	Integrated DNA Technologies Germany GmbH	N/A
Primer: Glis2 Forward: GACGAGCCCCTCGACCTAA Reverse: AGCTCTCGATGCAAAGCATGA	Integrated DNA Technologies Germany GmbH	N/A
Primer: Hprt Forward: GCAGTACAGCCCCAAAATGG Reverse: AACAAAGTCTGGCCTGTATCCAA	Integrated DNA Technologies Germany GmbH	N/A
Primer: IL1β Forward: TATCACTCATTGTGGCTGTGGA Reverse: CATCTCGGAGCCTGTAGTGC	Integrated DNA Technologies Germany GmbH	N/A
Primer: IL6 Forward: GCTACCAAACTGGATATAATCAGGA Reverse: CCAGGTAGCTATGGTACTCCAGA	Integrated DNA Technologies Germany GmbH	N/A
Primer: Rplp0 Forward: TCGGGTCCTAGACCAGTGTTC< Reverse: AGATTCGGGATATGCTGTTGGC	Integrated DNA Technologies Germany GmbH	N/A
Primer: Thrb1 Forward: ACACCTTATCCAGGCCACTT Reverse: GTGGTACCCTGTGGCTTTGT	Integrated DNA Technologies Germany GmbH	N/A
Primer: TNFα Forward: TCTCATCAGTTCTATGGCCC Reverse: GGGAGTAGACAAGGTACAAC	Integrated DNA Technologies Germany GmbH	N/A
Software and algorithms		
GraphPad Prism 8.0 and 9.0	GraphPad	N/A
ImageJ 1.54b	ImageJ	N/A
Microsoft Excel 365	Microsoft	N/A
Minispec Plus Software 6.0	Bruker Corporation	N/A
NIS Elements Imaging Software 4.30	Nikon	N/A
NormFinder	MOMA	https://www.moma.dk/software/normfinder
QuantStudio Design & Analysis Software 1.5.1	Thermo Fisher Scientific	www.thermofisher.com/de/de/home/global/forms/life-science/quantstudio-3-5-software.html
SPECTROstar Nano - Data Analysis 3.01 R2	BMG Labtech	N/A
TSE PhenoMaster software V5.8.1, V6.2.0 and V6.5.3	TSE Systems	N/A
GraphPad Prism 8.0 and 9.0	GraphPad	N/A
Other		
AccuCheck Aviva	Roche	N/A
minispec Live Mice Analyzer (LF110)	Bruker Corporation	N/A

(*Continued on next page*)

Continued

REAGENT or RESOURCE	SOURCE	IDENTIFIER
NanoDrop™	Thermo Fisher Scientific	Cat#ND-ONE-W
QuantStudio™ 3 Real-Time PCR System	Thermo Fisher Scientific	Cat#A28567
UNIPROTECT NG cabinet	Zoonlab GmbH	N/A

RESOURCE AVAILABILITY

Lead contact

Further information and requests for resources and reagents should be directed to and will be fulfilled by the Lead Contact, Jens Mittag (jens.mittag@uni-luebeck.de).

Materials availability

The Thrb knockout mouse line in this study has been made available previously from jax.org as strain #003462. The AAV8-TBG-mCherry or AAV8-TBG-mThrb1 are available at VectorBuilder with the catalog numbers AAV8M(VB220215-1039yuh) or AAV8L(VB211123-1086ztk).

Data and code availability

No code has been produced in this study. Data are available from the lead contact, Jens Mittag (jens.mittag@uni-luebeck.de). The data on non-specificity of thyroid hormone receptor antibodies mentioned in the limitations section of the study are available from FigShare: https://doi.org/10.6084/m9.figshare.24145185.v1.

EXPERIMENTAL MODEL

Animals

TRβ knockout mice,[22,23] lacking both TRβ isoforms, and controls were bred on the C57Bl/6NCrl background in the Gemeinsame Tierhaltung (GTH) University of Lübeck. Male animals at the age of 4–6 months were single housed at 30° ± 2°C with free access to food and water in a climate chamber (Zoonlab GmbH, Germany) with a constant 12-hour-light/12-hour-dark cycle for three weeks before receiving control diet (#E15668-043; Ssniff Spezialdiäten GmbH, Germany) with calories provided by carbohydrates (72%), fat (16%) and protein (12%) or choline-deficient high fat diet (CD-HFD) (#S0585-E010; Ssniff Spezialdiäten GmbH, Germany) with a composition of carbohydrates (31%), fat (60%), protein (9%). Body composition was studied by nuclear magnetic resonance spectroscopy (NMR) (minispec LF110, Bruker Corporation, Germany). All animal experiments were carried out according to EU guideline regulations (210/63/EU) and approved by the MEKUN Schleswig-Holstein (Germany).

AAV gene therapy

Wild-type C57Bl/6NCrl mice were purchased from Charles River Laboratories (Charles River, Germany) and experiments were conducted at the age of 7 months. Animals were single housed at 30°C with food and water *ad libitum* and after one week received CD-HFD (#S0585-E010; Ssniff Spezialdiäten GmbH, Germany). For AAV, serotype 8 was used in combination with the human thyroxine binding globulin (TBG) promotor to ensure hepatocyte specificity. Animals were anesthetized by isoflurane and kept on a homeothermic monitoring system to maintain core body temperature, while 100 µL of AAV8-TBG-mCherry or AAV8-TBG-mThrb1 (VectorBuilder GmbH, Germany) with a final concentration of $1.33x10^{11}$ and $3.44x10^{11}$ viral particles per animal were administered via lateral tail vein injection, respectively. For mCherry detection, liver sections from unfixed OCT-coated frozen tissue were cut at 7 µm, fixed in 4% PFA for 20 min, then washed in PBS prior to antigen retrieval with sodium citrate buffer at 80°C. Primary antibody goat mCherry 1:500 (AB0040; OriGene Technologies GmbH, Germany) was left overnight at 4°C. Alexa 594 conjugated donkey anti-goat 1:400 (A11058; Invitrogen, Germany) was used as secondary antibody. All sections were stained with mounting medium with DAPI (Invitrogen, Germany).

METHOD DETAILS

Glucose and insulin tolerance test

Mice were fasted for 6 h with free access to water before intraperitoneal injection of D-(+)-Glucose (Sigma-Aldrich, Germany) 1.5 g/kg body weight in sterile 0.9% saline. Blood glucose was measured in tail blood before and 15, 30, 60, and 120 min post injection using a glucometer (AccuCheck, Aviva). Animals recovered for 2 days until an intraperitoneal injection of insulin (NovoRapid Penfill 100E/mL, Novo Nordisk) of 0.75 U/kg body weight for recording insulin tolerance, and blood glucose was recorded before and 15, 30, 60, 90, and 120 min post injection.

Indirect calorimetry

Oxygen consumption and carbon dioxide production were measured via indirect calorimetry using an open respirometry system (TSE PhenoMaster, TSE Systems). Mice were transferred to a climate chamber and provided with food and water *ad libitum*. Energy expenditure,

food and water intake, respiratory quotient (RQ = carbon dioxide produced/oxygen consumed) and activity were measured at 20-minute-intervals. Daily energy expenditure (DEE, kJ/day) was calculated using the RQ and the caloric equivalents given by[50] with (heat production (HP, mW) = (4.44 + 1.43 * RQ) * VO_2 (mL O_2/h)) of a 24 h interval. Analysis of the data was done using Microsoft Office Excel and TSE PhenoMaster software V6.5.3 (TSE Systems, Germany).

qPCR

RNA was isolated following the manufacturer's instructions using the miRNeasy mini kit including a DNase digestion (QIAGEN, Germany) step. cDNA synthesis was performed using the Molecular Biology ReserAid cDNA Kit (Thermo Fisher Scientific, Germany) from 1 μg of RNA. QuantStudio Applied Biosystems (Thermo Fisher Scientific, Germany) and GoTaq qPCR Master Mix (Promega, Germany) were used for qPCR analysis. Efficiency of qPCR primers was determined using standard curves and NormFinder (https://moma.dk/normfindersoftware, Denmark) was used to select the best combination of reference genes. Gene expression was normalized with *hypoxanthine phosphoribosyltransferase (Hprt)* and *ribosomal protein lateral stalk subunit P0 (Rplp0)* for liver tissue and *Hprt* and *peptidylprolyl isomerase A (Ppia)* for kidney using the $\Delta\Delta C_T$ method.

T3/T4 and C-peptide ELISA

Serum total triiodothyronine (T3) (DNOV053, NovaTec Immundiagnostica GmbH, Germany) and total thyroxine (T4) (EIA-1781, DRG Diagnostics, Germany) concentrations were determined with an ELISA according to manufacturer's instructions. Although the assays are certified for human total T3 and T4, they provide accurate results for mice as well.[51,52] Intrahepatic TH levels were determined as described previously by the Endocrine Laboratory Amsterdam UMC.[53] Serum C-peptide 2 (EZRMCP2-21K, Sigma-Aldrich, Germany) was determined with an ELISA according to manufacturer's instructions.

Clinical chemistry parameters

Serum activity of AST, ALT and intrahepatic triglycerides (Sigma-Aldrich, Germany) were determined according to the manufacturer's instructions.

Histology

Tissues were fixed in 4% paraformaldehyde (PFA) for 48 h and then dehydrated in increased concentrations of ethanol and xylol prior to paraffin embedding. For cryosections, tissues were fixed in 4% PFA overnight with subsequent cryoprotection in 15% sucrose overnight and 20% sucrose. 5 μm paraffin sections were stained for Hematoxylin and Eosin (H&E) using Mayer's hemalum solution (Sigma-Aldrich, Germany) and eosin Y solution 0.5% aqueous (Carl Roth GmbH&Co KG, Germany) according to manufacturer's instructions (X883.1, Carl Roth GmbH&Co KG, Germany). Sirius red 5 μm paraffin slides were stained for 60 min in Picrosirius solution, consisting of 0.1% of Direct Red 80 (Sigma-Aldrich, Germany) in picric aqueous solution 1.2% (AppliChem GmbH, Germany) post tissue rehydration, and then washed for 4 min in 0.5% acetic acid, dehydrated, cleared, and mounted. All sections were mounted with xylene-based mounting media (Leica Mikrosysteme Vertrieb GmbH, Germany). 7 μm thick cryosections were stained with Oil Red O (Sigma-Aldrich, Germany) according to manufacturer's instructions. Samples were frozen in optimal cutting temperature compound (Sakura Finetek Germany GmbH, Germany). Quantification of percentage of positive area was done using ImageJ 1.54b.

QUANTIFICATION AND STATISTICAL DETAILS

Microsoft Office Excel and GraphPad Prism 9 software were used (GraphPad Software, San Diego, USA). Data were analyzed using two-way ANOVA followed by post hoc tests or Student's *t* test. Values are represented as mean ± SD and the levels of significance are *$p < 0.05$, **$p < 0.01$, ***$p < 0.001$, ****$p < 0.0001$. Statistical details such as test type, p values and sample sizes are provided in Table S1.